

# The Universal Dynamics of Tumor Growth

Antonio Brú,\* Sonia Albertos,<sup>†</sup> José Luis Subiza,<sup>‡</sup> José López García-Asenjo,<sup>§</sup> and Isabel Brú<sup>¶</sup>

\*CCMA, Consejo Superior de Investigaciones Científicas, 28006 Madrid, Spain; <sup>†</sup>Servicio de Aparato Digestivo, Hospital Clínico San Carlos, 28003 Madrid, Spain; <sup>‡</sup>Servicio de Inmunología, Hospital Clínico San Carlos, 28003 Madrid, Spain; <sup>§</sup>Servicio de Anatomía Patológica, Hospital Clínico San Carlos, 28003 Madrid, Spain; and <sup>¶</sup>Centro de Salud La Estación, 45600 Talavera de La Reina, Toledo, Spain

**ABSTRACT** Scaling techniques were used to analyze the fractal nature of colonies of 15 cell lines growing in vitro as well as of 16 types of tumor developing in vivo. All cell colonies were found to exhibit exactly the same growth dynamics—which correspond to the molecular beam epitaxy (MBE) universality class. MBE dynamics are characterized by 1), a linear growth rate, 2), the constraint of cell proliferation to the colony/tumor border, and 3), surface diffusion of cells at the growing edge. These characteristics were experimentally verified in the studied colonies. That these should show MBE dynamics is in strong contrast with the currently established concept of tumor growth: the kinetics of this type of proliferation rules out exponential or Gompertzian growth. Rather, a clear linear growth regime is followed. The importance of new cell movements—cell diffusion at the tumor border—lies in the fact that tumor growth must be conceived as a competition for space between the tumor and the host, and not for nutrients or other factors. Strong experimental evidence is presented for 16 types of tumor, the growth of which cell surface diffusion may be the main mechanism responsible in vivo. These results explain most of the clinical and biological features of colonies and tumors, offer new theoretical frameworks, and challenge the wisdom of some current clinical strategies.

## INTRODUCTION

Tumor growth is a complex process ultimately dependent on tumor cells proliferating and spreading in host tissues. The search for the underlying mechanisms of tumor development and progression has been largely focused on the molecular changes accounting for the malignant phenotype at the cell level, while our knowledge on tumor growth dynamics has remained scarce. In part, this has been due to difficulties in developing tools able to describe growth processes associated with disordered phenomena. As with many natural objects, cell colonies are fractal (Losa et al., 1992; Cross et al., 1995; Losa, 1995), and a description of their very complex contours using classical Euclidean geometry is very difficult to provide. However, the contours of objects can give valuable indications about their dynamic behavior, and the fractal nature of the contours of tumors/cell colonies—with their scale invariance (self-affine character)—allow scaling analysis to be used to determine this.

A very important implication of the spatial and temporal symmetries of tumors is that certain universal quantities (termed critical exponents) can be defined which allow the characterization of tumor growth dynamics. In turn, this allows the main physical mechanisms responsible for their growth processes to be determined.

The current view of tumor growth kinetics is based on the general assumption that tumor cells grow exponentially (Shackney, 1993). Such kinetics agrees with the unlimited proliferative activity of tumor cells recorded in early, mainly in vitro, studies. However, a number of poorly explained issues remain in disagreement with an exponential regime of

cell proliferation. For example, there is an evident discrepancy between the exponential tumor growth theory and experimental data obtained from tumor cells growing in vivo: tumor doubling times have been found to greatly exceed cell cycle times. Lower-than-expected activity of tumor cells and greater-than-expected aneuploidy have also been consistently found. These issues are of great importance since both radiotherapy and chemotherapy are entirely based on cytokinetics.

In a previous article (Brú et al., 1998) we mathematically described the growth dynamics of colonies derived from a tumor cell line (rat astrocyte glioma C6), which raised reasonable doubts about the exponential cell proliferation theory. The novel approach used in this study was based on fractality (Mandelbrot, 1982) and scale invariance of the colony contour. These cells form colonies that are fractal objects which can be characterized by a fractal dimension (a measure of their degree of complexity). This allows the use of scaling analysis (Mandelbrot, 1982; Barabási and Stanley, 1995; Brú et al., 1998) for determining their dynamic behavior, which was found compatible with the molecular beam epitaxy (MBE) universality class (Brú et al., 1998).

In the present study, different cells lines and different types of solid tumor were studied to determine whether such growth dynamics also apply to them. In the case of cells cultivated in vitro, all cells growing as colonies have dynamics compatible with the MBE universality. These dynamics are characterized by: 1), a linear growth rate, 2), the constraint of growth activity to the outer border of the cell colony or tumor, and 3), diffusion at the colony surface. In this work, the term “linear” means that the colony radius grows linearly with time. With respect to tumors growing in vivo, common characteristics were seen in all cases, several of which were common to those of tumors growing in vitro. In all cases, growth in these in vivo tumors was limited to the

Submitted June 27, 2002, and accepted for publication July 23, 2003.

Address reprint requests to Antonio Brú, Serrano 115, 28015 Madrid, Spain. Tel.: 34-91-7452500; E-mail: antonio.bru@ccma.csic.es.

© 2003 by the Biophysical Society

0006-3495/03/11/2948/14 \$2.00

tumor border (Figs. 6–8), which could indicate that the mechanisms at work *in vitro* are also those at work *in vivo*. The Discussion will provide clinical and biological evidence that this is the case.

As shown in this article, any type of tumor developing *in vivo* has most of its cell proliferation constrained to the border. This may indicate that cell surface diffusion is the main mechanism responsible for growth in any type of tumor.

## MATERIALS AND METHODS

### Cell lines

Cell lines were obtained from the Servicio de Inmunología, Hospital Clínico San Carlos (Madrid, Spain) and from ATCC (American Type Cell Culture, Rockville, MD).

### Cell colonies

Cell colonies were formed in 5-cm-diameter petri dishes by shedding disaggregated cells at low density (1000 to 5000 cell/ml) in a culture medium that completely covered them. The medium employed for HT-29, HeLa, 3T3, 3T3 K-ras, and 3T3 V-src cell lines was RPMI 1640, 2mM L-glutamine, 80  $\mu\text{g/ml}$  gentamicin, and 10% fetal bovine serum (FBS). For the C6 cell line, a mixture of Dulbecco modified Eagle medium (DMEM) and F12 Ham's mixture (F12) in a 1:1 ratio supplemented with 10% FBS was used; for MCA3D, AT5 and Car B was supplemented with Ham's mixture and 10% FBS. For HT-29 M6, C-33 A, Saos-2, VERO C, and Mv1Lu, DMEM supplemented with 10% FBS was employed. After 48 h of culture, various individual clones containing 4–8 cells were chosen for study. Cultures were maintained in a 5% CO<sub>2</sub> atmosphere at 37°C, carefully changing half of the culture medium every three days.

### Tumor sections

All human tumors were spontaneous tumors surgically removed from human patients at the Hospital Clínico San Carlos (Madrid, Spain). Tissue sections (4  $\mu\text{m}$  thick) were obtained from paraffin-embedded material on poly-L-lysine-coated glass slides. After deparaffinization and rehydration, the sections underwent microwave treatment three times for 5 min. Endogenous peroxidase activity was blocked with hydrogen peroxide for 15 min. Sections were incubated with Ki-67 (MIB-1, diluted 1:50; Immunotech, Marseille, France) for 1 h at room temperature; they were then incubated with biotinylated secondary antibody for 20 min, followed by treatment with streptavidin-biotin-peroxidase complex (LSAB kit, Dako, Milan, Italy) for 20 min at room temperature. The sections were rinsed with several changes of phosphate-buffered saline (PBS) between steps. Color was developed with diaminobenzidine tetrahydrochloride. Light counterstaining was performed with hematoxylin.

### Bromodeoxyuridine labeling

Cell cultures were pulsed with bromodeoxyuridine (BrdU) (10  $\mu\text{M}$ ) for 1 h at 37°C. After washing with prewarmed Hanks' balanced salt solution, cells were fixed (8 min) with methanol:acetone (2:1) at –20°C, washed with PBS, and submitted to further incubation (1 h) with 1M HCl. BrdU was immunodetected by means of anti-BrdU specific antibodies, using a secondary antibody coupled with peroxidase and the diaminobenzidine tetrahydrochloride-substrate chromogen system.

### Counting procedure

Ki-67 positive cells were defined as having brown nuclear staining. Ki-67 score was expressed as the percentage of positive cells relative to the total

number of tumor cells. For each slide, the number of positive cells was counted. These evaluations were performed without knowledge of clinicopathological data.

### Image processing

Colonies were photographed at 24-h intervals during the study (for over 1400 h in some cases) using an inverted phase-contrast microscope (Diaphot, Nikon, IZASA S.A., Madrid, Spain). Cell colonies showing adhering growth were considered as two-dimensional systems. Photographs were scanned with a final resolution of 1.3  $\mu\text{m/pixel}$ . Cell colony profiles were hand-traced. Scaling analysis and other measurements were then performed on these profiles with in-house computer software.

### Determination of the fractal dimension of interfaces

To determine the fractal dimension value, data were treated using three different methods: the box counting method, the yardstick method, and the  $y/x$ -variance relationship. As expected, for any given interface, total coincidence between the three methods was found.

### Fractals and scaling analysis

In a previous article (Brú et al., 1998), we established the fractal nature of the contours of rat astrocyte glioma C6 colonies and used scaling analysis to show that the colony growth dynamics belonged to the MBE class. The analysis of tumor/colony contours was based on the fractal geometry established by Mandelbrot (1982), and on the scale invariance of fractal interfaces. The same techniques are used in the present paper to show that all tumors/colonies have these same dynamics.

Fractal interfaces—for example, those shown in Fig. 1 which correspond to different culture times of a HeLa cell colony—show temporal and spatial invariances during the process of roughening. The increase in irregularity of a front—or roughening (roughness is a useful quantitative measurement of

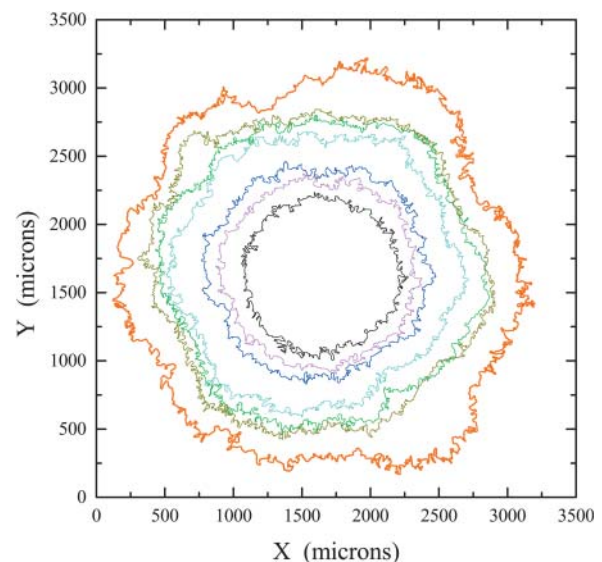


FIGURE 1 Cell colony contours. Contours of a C6 cell line at different culture times. Morphology of tumor contours determines the dynamic behavior of growth by means of the scale invariances of their complex structures.

the irregularity of an interface such as that of a tumor or cell colony contour—is generally analyzed in terms of a time- and position-dependent function called the “local width function” or “interface width,”  $w(l,t)$ . This is defined as the root mean square of the deviations of an interface about its mean value and is defined by the relationship

$$w(l,t) = \left\{ \frac{1}{N} \sum_{i=1}^N [r_i(t) - \langle r_i \rangle_l]^2 \right\}^{1/2} \quad (1)$$

as a function of the arc length  $l$  and the time  $t$ , where  $L$  is the length of the whole contour,  $r_i$  the distance from the center of the tumor mass to the point  $i$  of the interface, and  $\langle r_i \rangle_l$  the average radius of the arc length (Fig. 2). The term  $\langle \cdot \rangle_l$  is the local average of subsets of arc length  $l$ , and  $\{ \cdot \}_L$  is the overall average of the system (Brú et al., 1998).

As a result of the fractal nature of the interface—or the cell colony contour—the interface width possesses a series of both spatial and temporal invariances which provide the basis for scaling analysis (see Appendix A). All these invariances exhibit power law behavior, and for each type of invariance a critical exponent can be defined as the power law exponent. The power law behavior arises from the dependence of the interface width on the observation length and timescales. Usually, these interfaces become more and more rough as time goes by until, in some cases, the interfaces are always of the same roughness—they reach saturation.

How this roughening process develops both in time and in space is described by five critical exponents. Two of these exponents are related to the geometry of the system, quantifying its roughness on two scales: at the small scale of the system, i.e., the local roughness critical exponent  $\alpha_{loc}$ , and at system size scale, i.e., the global roughness critical exponent  $\alpha_{glob}$ . The third exponent is related to the development of the interface width with time:  $\beta$ , the growth exponent. A further exponent is the dynamic exponent,  $z$ , which is related to the correlation time of the interface. The physical meaning of this exponent is related to the celerity by which the information about points growing on the interface is transmitted across the interface. Finally, when the development of the interface is anomalous from a dynamic point of view, it is defined by another growth exponent,  $\beta^*$ , which describes this anomaly in time. By determining this set of five exponents, which are not independent (see Appendix A), the dynamics of the interface can be known, as well as the main mechanisms responsible for growth. The dynamics of a process is written in its interface, and this information can be extracted by determining these critical exponents.

All known dynamic processes have been classified into just a few universality classes, each comprising all those physical processes with the same type of dynamics, and each characterized by having a different set of values for this series of critical exponents. Further, each universality class

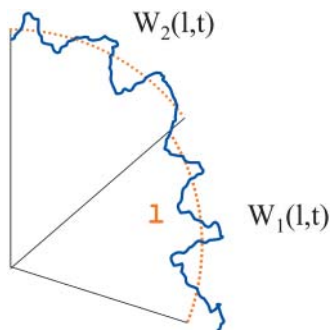


FIGURE 2 Interface width of a tumor or cell colony border. The interface width is calculated for sectors with an arc length  $l$ . For each arc length, the mean value of the interface and the fluctuations around it are calculated to obtain the corresponding interface width. For a given value of the length of a sector, all values of the interface width are averaged to obtain the final value of the arc length  $l$ ,  $w(l,t)$ . The power law behavior of  $w(l,t)$  versus  $l$  provides the local roughness critical exponent.

reflects the main conditioning factor responsible for growth, which can be described by a continuum stochastic equation.

## RESULTS

### Fractality of contours

The first condition that must be fulfilled to apply scaling analysis techniques is that the growth behavior of a process lie in the fractal nature of the interface.

The contours of a series of colonies of different cell lines and tumors were morphometrically analyzed to calculate their geometric dimensions (Tables 1 and 2) (see Materials and Methods). In all cases, a noninteger value, i.e., a fractal dimension ( $d_f$ ), was found. The values lay in the range 1.05–1.30, characteristic of any fractal object. These values are in good agreement with previous determinations of the fractal dimensions in melanomas and skin lesions (Claridge et al., 1992; Cross et al., 1995). The complexity of the contours of both colonies and tumors is due to the complexity of the growth process rather than the individual characteristics of the cells that compose them. In all the tumors/colonies studied, the dynamics were the same, and, therefore, fractal dimensions do not seem to depend on the morphological characteristics of the cells but rather on the growth process. The differences found in the fractal dimensions might be related to the growth medium (in vivo versus in vitro) or to specific conditions in the culture or of the growth process.

During colony growth, the value of  $d_f$  remained constant in all the cell lines studied. It is remarkable that the cell line HT-29 (colon adenocarcinoma) had an in vitro fractal dimension of 1.12 and a corresponding in vivo value of 1.30 (Tables 1 and 2). This difference indicates the greater complexity of the host tissue wherein tumors grow compared to the culture medium in which cell colonies are cultivated (much more homogeneous). From these results, the fractality of all the tested cell lines and tumors was established, and contour fractality allowed scaling techniques to be used to obtain growth dynamics.

### Growth dynamics

The dynamics and basic mechanisms of growth processes can be fully described by the set of five critical exponents determined by scaling analysis. Two of these exponents are directly related to the border's shape: local roughness,  $\alpha_{loc}$ , and global roughness,  $\alpha_{glob}$ . The other three are related to the development over time of the contours:  $\beta$  and  $\beta^*$  (the growth exponents), and  $z$  (the dynamic exponent).

The 15 cell lines were grown in culture to determine the critical exponents of their colony contours by analyzing them at intervals of 24 h. In all cases, the following characteristic values were obtained (Figs. 3 and 4):  $\alpha_{loc} = 0.9 \pm 0.1$ ,  $\alpha_{glob} = 1.5 \pm 0.15$ ,  $\beta = 0.38 \pm 0.07$ ,  $\beta^* = 0.15 \pm 0.05$ , and  $z = 4.0 \pm 0.5$  (Table 1). These values indicate that the

**TABLE 1 In vitro cell lines**

Cell line	Type	Origin	$d_f$	$\alpha_{loc}$	$\alpha_{glob}$	$\beta$	$z$	$\beta^*$	Growth rate ( $\mu\text{m/h}$ )
HT-29	Colon adenocarcinoma	Human	1.13	0.91	1.51	0.38	3.9	0.15	1.93
HT-29 M6	Mucus secreting HT-29 cells	Human	1.12	0.91	1.47	0.37	3.9	0.14	1.85
C-33 <sup>a</sup>	Cervix carcinoma	Human	1.25	0.89	1.48	0.36	4.1	0.14	6.40
Saos-2	Osteosarcoma	Human	1.34	0.92	1.50	0.37	4.0	0.14	0.94
AT5	Primary human foreskin fibroblasts	Human	1.23	0.91	1.48	0.37	4.0	0.14	8.72
HeLa	Cervix carcinoma	Human	1.30	0.90	1.47	0.39	3.7	0.15	1.34
3T3	Mouse fibroblasts	Animal	1.20	0.90	1.51	0.37	4.0	0.15	1.10
3T3 K-ras	Transformed mouse fibroblasts	Animal	1.32	0.91	1.52	0.39	3.8	0.16	1.89
3T3 V-src	Transformed mouse fibroblasts	Animal	1.34	0.90	1.50	0.38	3.9	0.15	1.35
VERO C	African green monkey kidney cells	Animal	1.18	0.92	1.50	0.38	3.9	0.15	5.10
Car B	Mouse spindle carcinoma	Animal	1.20	0.93	1.51	0.37	4.1	0.14	2.06
MCA3D	Mouse keratinocytes	Animal	1.09	0.89	1.52	0.39	3.9	0.16	3.73
Mv1Lu	Mink, lung epithelial cells	Animal	1.23	0.90	1.52	0.36	4.2	0.15	11.50
B16	Mouse melanoma	Animal	1.13	0.93	1.55	0.37	4.2	0.13	5.83
C6	Rat astrocytoma	Animal	1.21	0.91	1.49	0.37	4.0	0.14	2.90

The in vitro growth of individual cell clones was studied by analyzing colony contours every 24 h.  $d_f$  is the fractal dimension measured by the box-counting method. The errors in  $d_f$ ,  $\alpha_{loc}$ ,  $\alpha_{glob}$ ,  $\beta$ ,  $z$ , and  $\beta^*$  are  $\pm 0.03$ ,  $\pm 0.05$ ,  $\pm 0.15$ ,  $\pm 0.08$ ,  $\pm 0.5$ , and  $\pm 0.08$ , respectively. The error of growth rate is  $\leq 0.01 \mu\text{m/h}$ . From the values of fractal dimensions, no geometrical difference between tumoral and nontumoral cell lines and between tumoral cell lines depending on their origin, species, or accumulated genetic changes could be established.

growth dynamics of cell colonies correspond to the MBE universality class (Das Sarma et al., 1994) ( $\alpha_{loc} = 1.0$ ,  $\alpha_{glob} = 1.5$ ,  $\beta = 3/8$ ,  $\beta^* = 1/8$ , and  $z = 4.0$ ). This is described by the following linear continuum equation (Das Sarma et al., 1994; Brú et al., 1998; Kessler et al., 1992):

$$\frac{\partial h(x, t)}{\partial t} = -K \frac{\partial^4 h(x, t)}{\partial x^4} + F + \eta(x, t), \quad (2)$$

where  $h(x, t)$  is the position on the tumor or colony border,  $K$  is the surface diffusion coefficient (which is independent of critical exponents),  $F$  is the growth rate, and  $\eta(x, t)$  is random

noise where  $\langle \eta(x, t) \rangle = 0$  and the correlation  $\langle \eta(x, t) \eta(x', t') \rangle = 2D\delta(x-x')\delta(t-t')$  is seen. The first term on the right side of the equation implies that the growth process is characterized by the surface diffusion of cells (Brú et al., 1998).

Host-tumor interfaces were used to calculate the values of local ( $\alpha_{loc}$ ) and global ( $\alpha_{glob}$ ) roughness for the 16 tumor types investigated. These values were characteristically  $0.9 \pm 0.1$  and  $1.5 \pm 0.15$ , respectively. The time-related critical exponents ( $\beta$ ,  $\beta^*$ , and  $z$ ) could not be calculated for obvious reasons.

These values of the critical exponents of tumor roughness do not agree with the theoretical values of the MBE universality class in 2+1 dimensions for linear systems and in which the system size does not change. However, it must be taken into account that, in this case, there are two very important qualitative differences that could cause the values of the exponents to vary: the symmetry of the system is circular, not linear, and the system size varies with time. Presently, the values that would be obtained for the critical exponents in the latter case are unknown and require investigation in future work. In any event, as the following section shows, both experimental and clinical evidence indicate that, for tumors in vivo, the dynamics behaves as though the main mechanism responsible for growth were cell diffusion at the interface. Therefore, in both cases, a growth pattern characterized by the following can be foreseen:

1. Cell diffusion at the colony or tumor borders;
2. Cell proliferation mainly restricted to the colony or tumor border, i.e., growth is greatly inhibited inside the colony or tumor;
3. A linear growth rate for both colonies and tumors.

**TABLE 2 Human and animal tumors**

Type	Origin	$d_f$	$\alpha_{loc}$	$\alpha_{glob}$
Colorectal adenocarcinoma (protruded)	Human	1.29	0.90	1.57
Colorectal adenocarcinoma (excavated)	Human	1.17	0.89	1.39
Thyroid carcinoma	Human	1.05	0.90	1.34
Melanoma	Human	1.35	0.78	1.40
Lung epidermoid carcinoma	Human	1.19	0.94	1.40
Mammary adenocarcinoma	Human	1.31	0.89	1.41
Mammary nodal metastases	Human	1.31	0.89	1.43
Melanoma nodal metastases	Human	1.06	0.89	1.42
Gallbladder adenocarcinoma	Human	1.27	0.95	1.37
Basocellular carcinoma	Human	1.25	0.93	1.45
Colorectal adenoma	Human	1.10	0.95	1.53
Gastric adenocarcinoma	Human	1.21	0.95	1.33
Vocal chord epidermoid	Human	1.23	0.93	1.42
Esophagus adenocarcinoma	Human	1.20	0.91	1.30
FibroEhrlicht	Animal	1.27	0.94	1.47
Colon adenocarcinoma	Animal	1.19	0.91	1.43

Tumor contours were analyzed and their critical exponents  $\alpha_{loc}$  and  $\alpha_{glob}$  determined, as well as their fractal dimension  $d_f$  measured by the box-counting method. The errors in  $d_f$ ,  $\alpha_{loc}$ , and  $\alpha_{glob}$  were  $\pm 0.05$ ,  $\pm 0.15$ , and  $\pm 0.03$ , respectively.

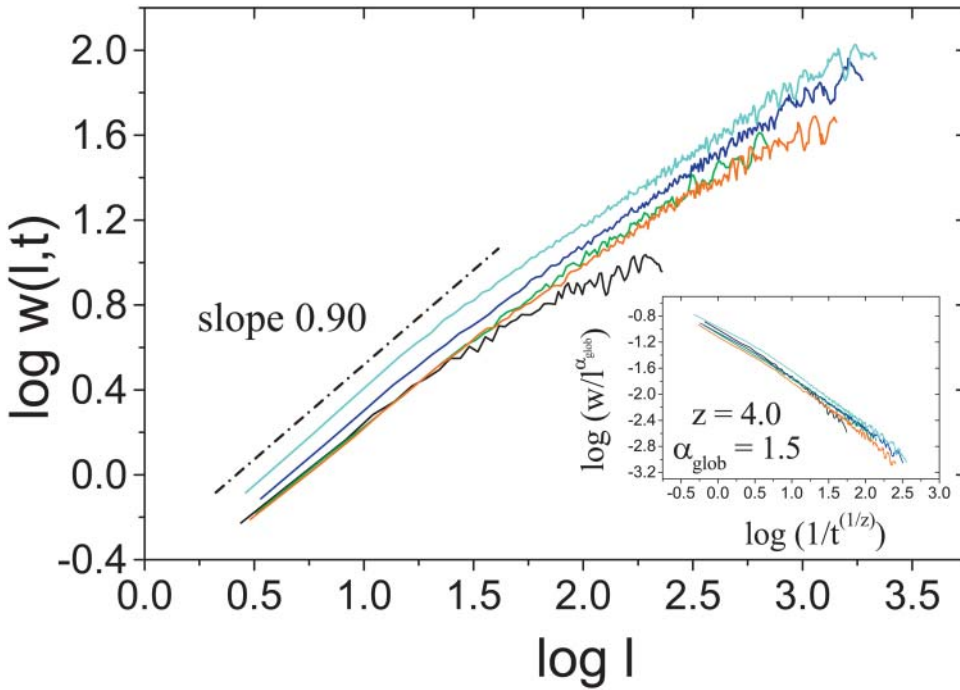


FIGURE 3 Scaling analysis of the colony interface width. The interface width is shown against window size for the HT-29 (colon adenocarcinoma) cell line at different times ( $t = 288$  h (black), 624 h (green), 986 h (red), 1203 h (blue), and 1348 h (cyan)). From the shape, the value of the local roughness exponent  $\alpha_{\text{loc}} = 0.91 \pm 0.10$  is obtained. In the inset of this figure, the transformation of  $w(l,t)$  into  $w(l,t)/l^\alpha$  and  $l$  into  $l/t^{(1/z)}$  shows that these curves collapse into a single, universal curve with  $z = 4.0$  and  $\alpha_{\text{glob}} = 1.5$ .

**Experimental assessment of the features imposed by MBE class dynamics**

*Cell surface diffusion*

MBE dynamics implies surface diffusion of cells, i.e., *their movement along the tumor/colony border, not their free movement away from it*. This should not be entirely surprising since cell movement is a well-known phenome-

non, as is the increase in motility of tumor cells. However, the diffusion associated with MBE dynamics is not random, but more frequent toward places where there is a large coordination number (in this case derived from the number of cells that surround a given cell). Therefore, diffusion to zones with greater local curvatures, i.e., with larger coordination numbers, should be expected. Preliminary studies recording cell colonies by time lapse video suggest

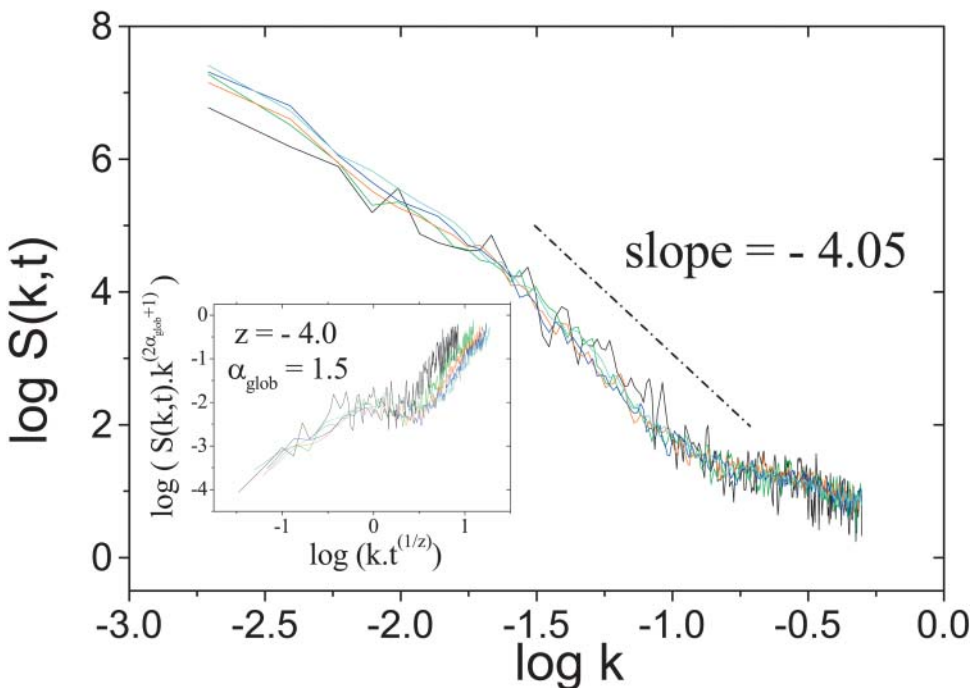


FIGURE 4 Scaling analysis of the colony power spectrum. This figure shows the structure factors of an HT-29 (colon adenocarcinoma) cell line at different times ( $t = 288$  h (black), 624 h (green), 986 h (red), 1203 h (blue), and 1348 h (cyan)). The global roughness exponent is obtained from the shape of these curves ( $2\alpha_{\text{glob}} + 1 = -4.0$ ), which gives a value for this critical exponent of 1.5. Transforming  $S(k,t)$  into  $S(k,t)k^{2\alpha+1}$  and  $k$  into  $k \cdot t^{(1/z)}$ , these curves collapse into a single universal curve as seen in the inset of this figure, with  $z = 4.0$  and  $\alpha_{\text{glob}} = 1.5$ .

that, at least for HT-29 cells, this is the case (Fig. 5). However, more work is needed to address the biomolecular features of this, especially since it constitutes the main mechanism of colony and tumor proliferation.

#### *Cell proliferation is restricted to the colony or tumor border*

To experimentally support this second characteristic of MBE dynamics, actively proliferating cells within colonies and tumors were labeled with bromodeoxyuridine (BrdU) and Ki-67, respectively. Fig. 6 shows a representative colony labeled after 260 h of culture. The proliferative activity was located mainly within the external portion. It must be borne in mind that at this time the greater part of the colony is not inhibited. This is confirmed by the velocity curve. However, a clear tendency toward the restriction of cell proliferation to the edge of the colony was seen. Thus, the outer region occupied 20% of the colony's surface but included 47% of all proliferating cells. Fig. 7 shows that cell proliferation is further restricted to the colony border in HeLa cells grown over a longer period (380 h). Similar results were obtained when analyzing tumor specimens (Figs. 8 and 9). Active Ki-67 cells were clearly concentrated in the external portion of tumors. Fig. 8 represents a colon adenocarcinoma. In this case, 80% of the active cells were found in the outer 20% of tumors; only 6% were found in the innermost 50% of the tumor. This constraint of cell proliferation to the border was also obtained even for polypous carcinomas. Figs. 6 c; 7, *bottom*, 8 c; and 9 show that, in every case, the number of proliferating cells increases as a function of the colony or tumor radius. This indicates a relationship between the ability to proliferate and spatial distribution within the colony or tumor. As a consequence, these data also indicate that proliferation is inhibited in the innermost areas.

#### *Linear growth rate*

In all studied cases, tumor radius grows linearly with time. The growth rate of colonies was obtained by plotting the variation of the mean radius as a function of time.

Common to all cell lines, colony growth was dominated by a linear growth regime throughout the culture period (up to 1400 h). This regime is, in most cases, preceded by an exponential transitional phase lasting 200 h on average. The slope of the linear regime indicates the average growth velocity of the colony, which was different depending on the cell line (Table 1) and growth substrate (not shown). It is important to note that the mean growth velocity of the colonies is characteristic of the process, and not of the cell line. It probably depends on a variety of external factors such as the experimental conditions, the available nutrients, type of medium, etc.

Changing the substrate did not modify the dynamic behavior, except for the average growth velocity. Fig. 9 shows the corresponding growth rate analysis of the HT-29

cell line. In this case, the exponential regime was one of the longest, lasting a little less than 400 h. Though exponential phases were shorter, similar results were found for all the cell lines studied. The inset of Fig. 9 shows the growth rate in semilogarithmic representation. It is not an exponential process; if it were, a straight line would be obtained.

In vivo tumor growth rate could not be measured directly as explained above. However, the restriction of cell proliferation to the tumor contour mathematically implies a linear growth rate.

## DISCUSSION

Elucidating the basic mechanisms of tumor growth is one of the most intricate problems in the field of tumor biology, and one of its major challenges. Many attempts have been made in recent decades to obtain a mathematical model that would allow us to discern these basic features of cell and tumor growth (Shackney, 1970; Durand, 1990; Gatenby and Gawlinsky, 1996; Byrne, 1997; Hart et al., 1998; Scalerandi et al., 1999; Drasdo, 2000; Kansal et al., 2000; Sherrat and Chaplain, 2001; Ferreira et al., 2002). Several different hypotheses have been postulated to describe the main conditioning factor of tumor growth, and nutrient competition between tumor cells or tumor and host cells is currently the most accepted. This concept of tumor growth is a legacy of an older problem, that concerning the growth of bacterial colonies. In the latter, it has been fully shown that the main mechanism is nutrient competition. However, this cannot be extrapolated to tumor growth. First, the majority of these models reproduce patterns with a roughness exponent of  $\alpha_{loc} = 0.5$ , which is in good agreement with the Eden model (Eden, 1961). Second, the kinetic behavior that reproduces these models is Gompertzian. However, it should be mentioned that there is often no qualitative or quantitative comparison made of these models. The roughness of simulated patterns obtained from mathematical models that consider nutrient competition is largely in good agreement with that corresponding to the Eden model, i. e.,  $\alpha_{loc} = 0.5$ . Other types of mathematical models also partially reproduce some features of tumor growth. Nevertheless, the majority are very restrictive in their hypothesis or use a series of conditions that are insufficient to reproduce the main features of tumor growth.

This work provides a very extensive and detailed study of pattern morphology both of tumors and cell colonies. From the behavior of the corresponding contours, both in time and with length scales, and by applying scaling techniques, the dynamics and the main mechanism responsible for tumor growth can be extracted without the need of any hypothesis. This is one of the major advantages of scaling analysis. Scaling techniques used to analyze the fractal nature of cell colonies growing in vitro, and of tumors developing in vivo, showed them to exhibit exactly the same growth dynamics independent of cell type. These dynamics are compatible not

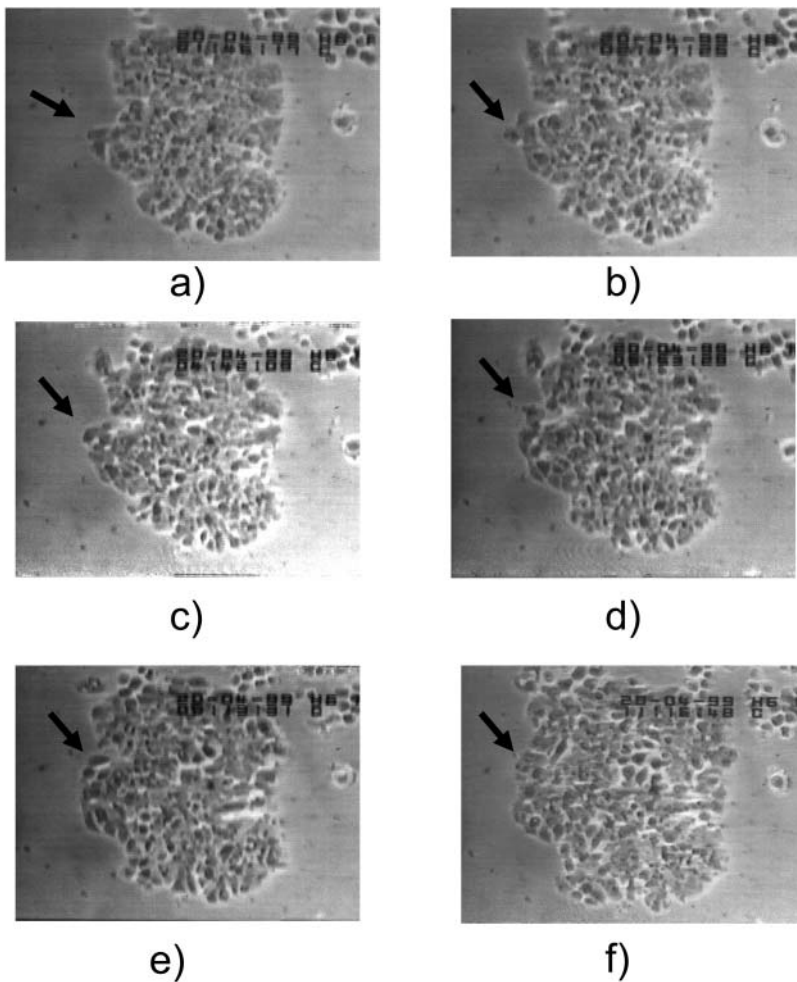


FIGURE 5 Cell surface diffusion. The dynamic behavior of cells growing in a colony is compatible with the molecular beam epitaxy universality class, of which surface diffusion is characteristic, i.e., cells located at the growing interface tend to migrate along the colony border. To show this movement, a clone of HT-29 cells formed after 300 h of culture was recorded by time lapse video. The figure shows different steps of this movement: (a) the arrow indicates a cell just after division; (b–e) the arrows follow this cell to show how it moves along the colony border; (e) the arrow shows the resting site of this cell at the interface. The local curvature radius is positive at the initial (a) and negative at the final (e) sites, consistent with predictions derived from molecular beam epitaxy dynamics and reflected experimentally for the first time here.

with the currently and widely accepted idea of Gompertzian growth, but with the MBE universality class, which involves a linear growth regime. It should be remembered that the concept of a Gompertzian growth regime is based on the exponential growth of cells, and an exponentially decaying growth rate is assumed. The Gompertz law is considered a robust feature of the nutrient-limited model of cancer growth. However, according to the present analysis, the main mechanism responsible for tumor progression would be cell diffusion at the tumor border.

Strikingly, the dynamics obtained for the studied tumors and cell colonies are the same for any cell proliferation process, independent of cell line or the in vivo or in vitro nature of growth. These dynamics, which are also obeyed in other phenomena such as crystal growth, possess the property of *super-roughness*. This means that the traditional Eden growth model (Eden, 1961), conceived to satisfy cell proliferation processes, does not explain tumor growth. The Eden model is the simplest growth model that can be defined based on random particle deposition and aggregation. The surface of an Eden cluster obeys scaling dynamics with  $\alpha_{\text{loc}} = \alpha_{\text{glob}} = 0.5$ . Far from this behavior, however, the

present results show that cell proliferation dynamics exhibit super-roughness ( $\alpha_{\text{glob}} \geq 1.0$ ) as an effect of surface diffusion, a process which tends to smooth the tumor or colony borders. The stochastic nature of duplication induces cell colony or tumor roughness, but this is generally counterbalanced by a smoothing or ordering process due to the mobility of generated cells. Cell diffusion on the tumor or colony border tends to counterbalance the effect of random duplication. There is, therefore, a mean doubling time (the duration of the cell cycle) with some dispersion around this value. Physically, this effect is described in Eq. 2 by the noise term.

In addition, as in the case of crystal growth where evaporation effects do not alter dynamic behavior in MBE universal dynamics, the movement of cells away from the colony/tumor does not influence the growth process.

The widely accepted concept of tumor growth kinetics is based on the assumption that tumor cells grow exponentially. However, it is generally recognized that this assumption is applicable to virtually no solid tumor growing in vivo (Shackney et al., 1978). Given an exponential-like growth regime, doubling times would be similar to the total duration

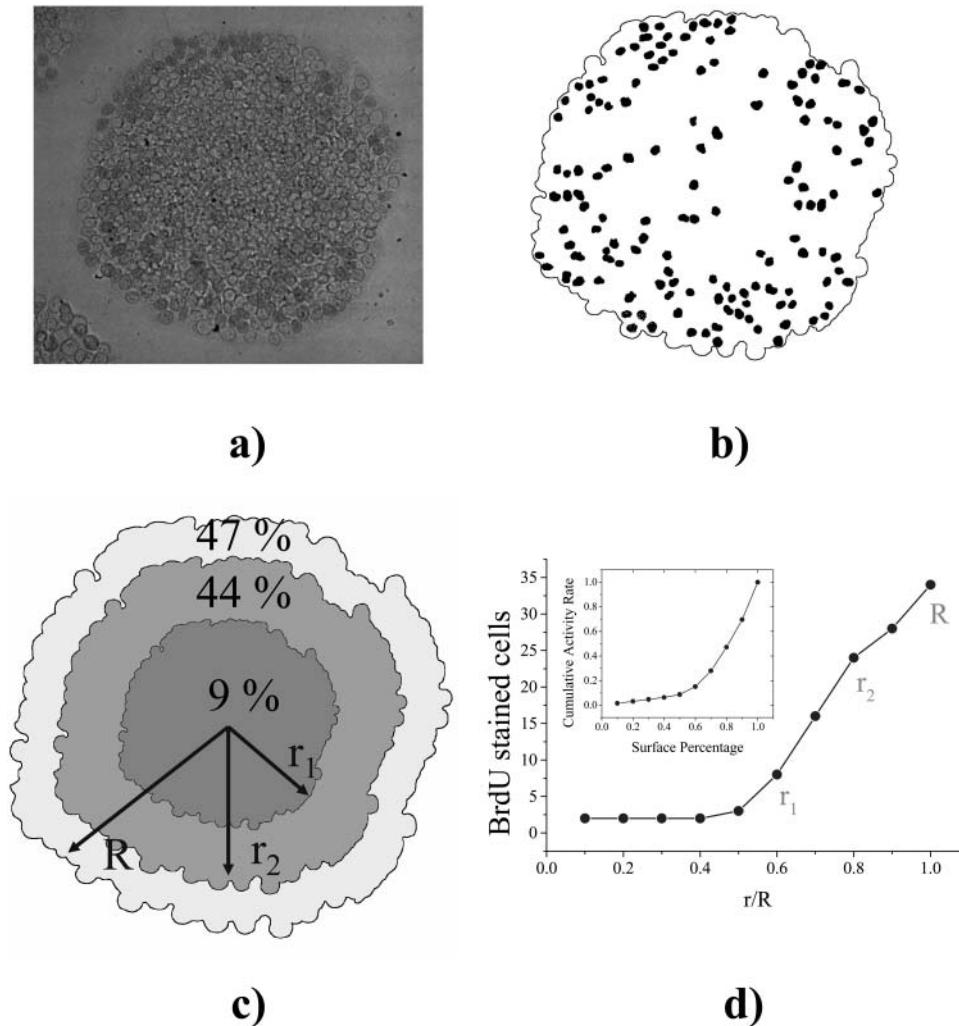


FIGURE 6 Spatial distribution of cell proliferation in colonies. (a) A clone of HT-29 cells formed after 260 h of culture and labeled with bromodeoxyuridine (BrdU). (b) Cells scored as BrdU positive. (c) Three different regions can be distinguished: an inner region of radius  $r_1 = R/2$  practically without activity, an intermediate region from  $r_1$  to  $r_2 = 0.8R$  with a linear increase in activity, and a third region from  $r_2$  to  $r_3 = R$  which has half of the whole colony activity. The outer region has 20% of the whole colony surface and 47% of total activity. (d) Various contours have been traced according to a division of the colony (from the center of its mass) into 10 inner contours of radii  $R/10, 2R/10, 3R/10, \dots, 9R/10$  and  $R$  (where  $R$  is the whole colony radius). Taking into account the number of BrdU stained cells, the spatial distribution of active cells is determined as a function of the radius. In the inset, the cumulative activity rate is plotted as a function of the colony surface. To a large extent, cell proliferation is seen to be located at the colony border. It is very important to note that (as seen in Fig. 4) for HT-29 line cells, a growing time of 260 h still corresponds to an exponential regime, in which contact inhibition is still very scarce. Only after 400 h does growth of the colony reach a linear regime with respect to the radius. From this moment, colony activity is constrained more and more to the border, as expected from its dynamics.

of the cell cycle. Nevertheless, tumor doubling times are strikingly longer than cell cycle times, e.g., more than 100-fold in breast carcinomas (Shackney, 1993). These differences are even more remarkable in large tumors. This is currently explained as a consequence of tumor cell loss and/or a low rate of cell production because of nutrient deprivation and/or waste product accumulation (Shackney, 1993).

Based on the results, it can be stated that tumor growth would be well described by a linear regime. It is then needless to account for the different incidental processes that might explain disagreements between a theoretical basis—the supposed exponential regime—and experimental observations which appear to show growth to be linear. It is important to again point out that, in this paper, a linear process means one in which rate changes with time in a completely linear way.

As already described, this linear regime implies that there are less actively proliferating cells, and that these are not randomly distributed throughout the whole volume of the tumor, but homogeneously constrained to the border. Only

when the colony is small enough to assume that most cells are located at the growing border is the growth regime depicted by an exponential—but still transient—phase.

Other than the growth dynamics of any type of tumor/colony being the same, the most important result of this study is perhaps that cell movement occurs at their surface. This type of movement (Fig. 5) invalidates the hypothesis that the main mechanism responsible for tumor growth is nutrient competition between cells. As seen in Fig. 10, newly generated cells move to sites with a higher coordination number, i.e., with a higher number of neighboring cells. This movement is that predicted by MBE dynamics and, from a mathematical point of view, is the movement originated by the fourth-order derivative in Eq. 2.

Tumors are surrounded by a very thin acidic environment as a result of cell metabolism (these cells mainly consume glucose and secrete lactic acid, increasing the acidity of the environment). Following the rules of cell surface diffusion as in MBE dynamics, the final position of a diffusing cell will be in a region in which the quantity of nutrients or oxygen is lower since it becomes surrounded by a greater number of

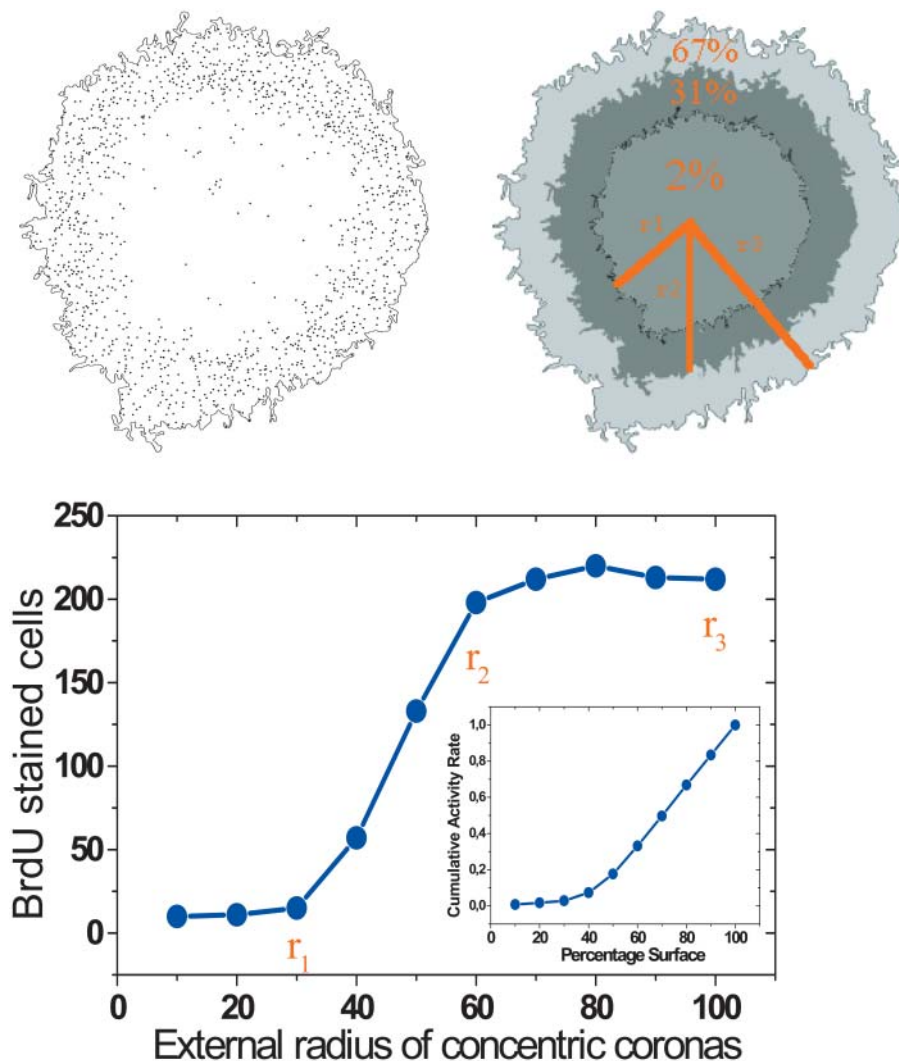


FIGURE 7 Spatial distribution of cell proliferation in colonies. As in Fig. 6, a spatial study of cell proliferation was made. This case corresponds to a HeLa cell line after 360 h of culture time. Cells in mitosis are stained brown. The three different regions in the figure contain 50%, 30%, and 20% of total tumor surface, respectively (inside to outside); cell proliferation is therefore mainly restricted to the border. As time progresses, cell proliferation will be more and more restricted to the colony border.

cells. Moreover, as a consequence of cell metabolism, the pH of this region will be lower than at the cell's initial position. The lack of oxygen in the concave regions where new cells deposit does not constitute an obstacle to tumor growth since cell proliferation is supported by anaerobic respiration (Eskey et al., 1993). Oxygen is a limiting factor only for functions such as differentiation, respiration, and mechanical work. This movement determines the mechanism responsible for the growth dynamics: as this work has determined both theoretically and experimentally, it is not possible to conceive tumor growth merely as a process of nutrient competition. On the contrary, this movement can be understood as the search for space by tumoral cells. In its initial position in Fig. 10, the mechanical pressure the new cell undergoes is greater than in its final position. This obliges that tumor growth be considered a process in which a mass grows and looks for space to avoid the mechanical response of both the host tissue and the immune response.

This has a number of consequences with respect to the treatment of solid tumors. First, the effectiveness of

chemotherapy becomes dependent on the specific surface of tumors. Given that the proliferating cells sensitive to antiproliferative agents are mainly associated with the surface of tumors, then the effectiveness of chemotherapy must decrease as tumor size increases. For this reason, the current log-kill concept of chemotherapy assumes a constant effect at random (Skipper et al., 1970), but it fails experimentally in large tumors (Shackney, 1970; Skipper et al., 1970). The concept of log kill rests on the fact that each chemotherapeutic cycle kills 90% of all cells in proliferation. But if proliferative cells are restricted to the border of the tumor and are not randomly distributed, as this work argues, the relative fraction of cells in proliferation compared to the total number of cells in the whole tumor is clearly much smaller. Chemotherapy would certainly kill all the cells on the border—but the inner cells, prevented from proliferating by the pressure exerted on them through the lack of space, would escape the effect of the therapeutic agent. They would therefore survive to become the new peripheral, proliferative, layer. However, their number would be again small in

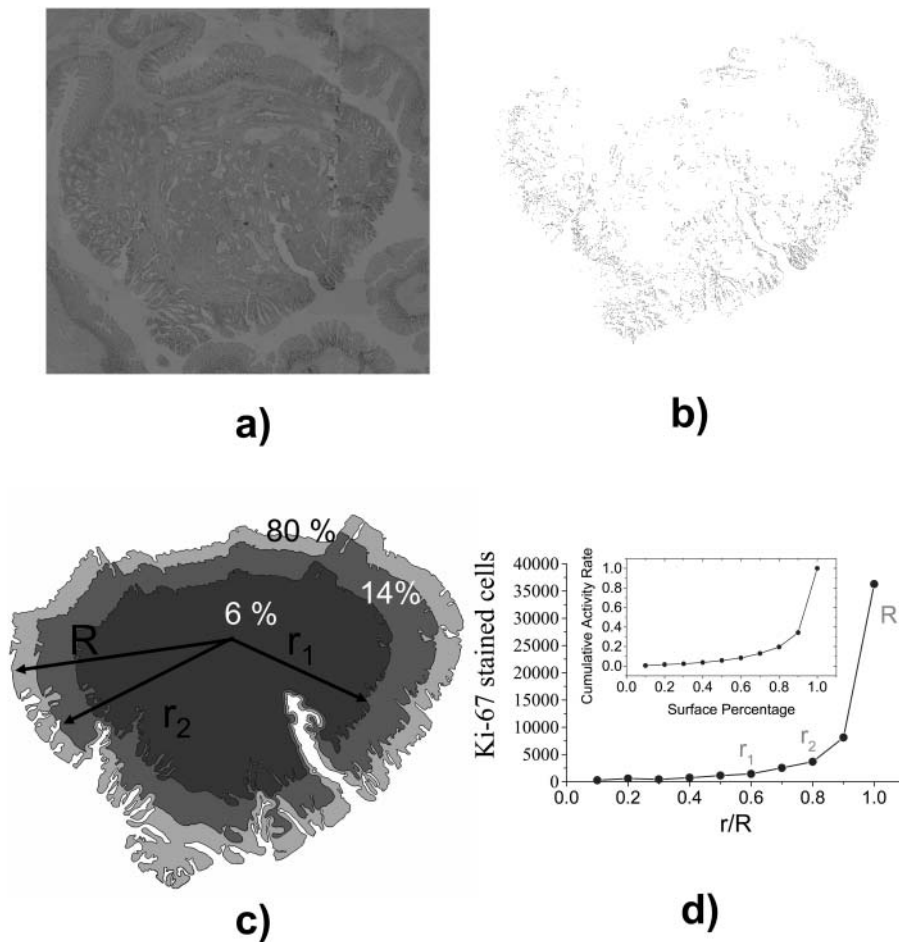


FIGURE 8 Spatial distribution of cell proliferation in tumors. (a) A human colon adenocarcinoma. (b) Cells scored as Ki-67 positive. (c) Tumor mass has been divided into three regions having 50%, 30%, and 20% of the whole tumor surface (inside to outside). The distribution of cell proliferation in these three regions (having a mean radius of  $R/2$ ,  $8R/10$ , and  $R$ , respectively,  $R$  being the mean radius of the tumor) is 6%, 14%, and 80%, respectively. (d) Various contours have been traced according to a division of the tumor (from the center of its mass) into 10 inner contours of radii  $r/10$ ,  $2r/10$ ,  $3r/10$ ,  $\dots$ ,  $9r/10$ , and  $r$  (where  $r$  is the whole tumor radius). Taking into account the number of Ki-67 stained cells, the spatial distribution of active cells is determined as a function of the radius. In the inset, the cumulative activity rate is plotted as a function of the colony surface. Spatial activity distribution corresponding to the three regions determined by  $r_1 = R/2$ ,  $r_2 = 8R/10$ , and  $r_3 = R$  is shown. Cell proliferation is mainly located at the tumor border, rather than randomly and homogeneously throughout the tumor as might be expected.

comparison to the total number of cells of the tumor—and so the process repeats itself. The efficacy of chemotherapy would be less than expected if all the cells in the tumor were randomly proliferating. It is important to note that both primary tumors and metastases show the same growth dynamics (Table 2). It is also well known that hypoxia is associated with resistance to radiation therapy and chemotherapy (Harris, 2002). This is also an important point to consider in developing therapy strategies if, following MBE dynamics, cells migrate to positions where they are more likely to suffer hypoxia (Figs. 5 and 10).

Second, aneuploidy (Caratero et al., 1990; Tomita, 1995), along with other genetic abnormalities (Sun et al., 1998; Ried et al., 1999), is more frequent than expected in advanced solid tumors, and less frequent in early stage than in advanced cancer. The genetic mutation rates in tumor cells are thought to be linked to the number of mitotic cell divisions (Nicholson, 1987). If an exponential growth regime is assumed, each cell must undergo 32 divisions to form a  $2 \text{ cm}^3$  tumor ( $\sim 4 \times 10^9$  cells). However, in a linear growth regime, the number of divisions by cells on the surface would be  $\sim 30$  times greater than at the center. Naturally, this leads to a higher frequency of genetic

abnormalities in cells at the growing tumor border. In this way, if we consider that metastases are generated from cells from the border of the primary tumor (Fukakawa, 1997), it is completely coherent that metastatic cells would be always more aneuploid than those of primary tumors. A linear growth regime provides a much better explanation of this than does exponential growth.

Another implication of a linear growth regime is that the most malignant cells should be located at the tumor border. This is because cells become more malignant as the number of chromosomal aberrations increases (Rasnick and Duesberg, 1999) (i.e., as the number of cell divisions increases). Given enough time, the accumulation of aberrations would probably lead to cell death, but tumors become mortal for the patient before this point is reached. Accordingly, the malignancy of cells should increase along the tumor radius: the further from the center, the more malignant the cell should be. One of the important clinical consequences of this is that it explains the discrepancy between anatomopathological analysis of biopsies and the diagnosis of many cancers. The doctor who performs the biopsy usually takes a sample from the center of the tumor to be sure that what is taken corresponds to the lesion. But if growth is linear, and

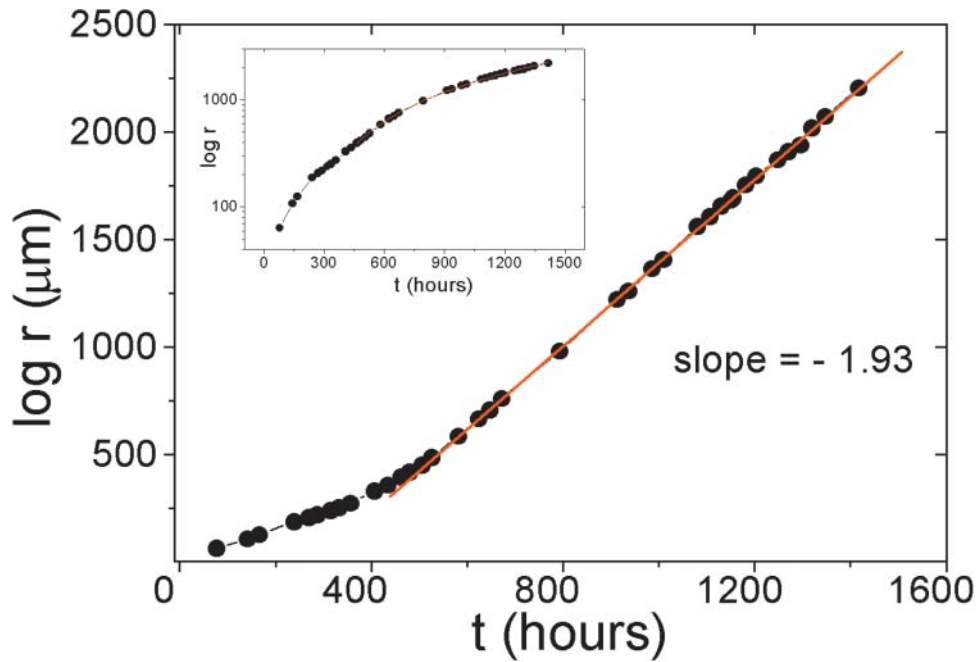


FIGURE 9 Colony growth. Development over time of the mean radius of a colony of HT-29 (colon adenocarcinoma) cells. The mean radius shows a linear regime with time (linear fit shown in red), which gives a constant interface speed of  $0.29 \mu\text{m/h}$ . This result is incompatible with the general assumption that tumors grow exponentially. An exponential regime is observed only at very early times, during which all cells are active. Later, in the linear regime, a very important cell fraction is partially contact-inhibited, and the majority of colony activity is constrained to a very fine band at the border, as suggested by the universal dynamic behavior determined for the growth process of any type of colony. This result supports the impossibility of the division of all cells in the colony, which would give an exponential regime for radius or size at any time.

the malignancy of cells increases along the tumor radius, such a biopsy would always take the least malignant cells and might lead to diagnostic error (Lieberman et al., 2000).

A major phenotypic hallmark of tumor cells is thought to be the lack of inhibition of the cell proliferation process. However, a downregulation of cell proliferation is shown by the present BrdU (for in vitro cell colonies) and Ki-67 (for in vivo tumors) labeling data (Figs. 7 and 8). Some type of inhibition of cell proliferation must therefore be operating on cells inside tumors. This has been observed experimentally on numerous occasions. Traditionally, it has been ascribed to necrosis, probably as a result of poor vascularization. In the present experiments, the same type of behavior is seen. However, at no time could the inhibition of proliferation have been due to central necrosis since none of the tumors became necrotic. Further, in the in vivo studies, no

correlation was found between the presence of blood vessels inside tumors and any increase in proliferation. However, the proposed model offers a new interpretation for the inhibition of cell proliferation inside tumors. The tumor contour is super-rough, indicating that tumors adopt the best shape for bearing the “pressure” exerted by the host organ and the inflammatory response, and it is these “pressure effects” that may be inhibiting proliferation of cells. Cells inside the tumor can proliferate if they have room to do so, but at the moment cell density becomes so high that there is no longer any space, inhibition begins. Durand (1990) showed that quiescent cells, when extracted from tumors and cultured, recover their proliferative capacity and resume their preinhibition cell cycle. This inhibition does not exist at the tumor border. The spatial distribution of mitotic cells in Figs. 6–8 fit a barometric distribution, i.e., an exponential distribution in good agreement with the argument derived from surface cell movement and the concept of tumor growth as a search for space. A growing tumor has therefore to release enough space at the host-tumor interface. This requirement is in line with the critical roles assigned in cancer invasion to the development of an acidic environment destroying parenchymal cells at the host-tumor interface (Gatenby and Gawlinsky, 1996) and/or the presence of tumor metalloproteinases cleaving the extracellular matrix (Sato et al., 1994; Egeblad and Werb, 2002), and also with the notion that tumor cells require enough motility to invade—growing cells cannot simply be pushed along a solid substratum to which they are adhered (Abercrombie, 1979). Thus, the dynamics, which has been verified in all studied cases, predict that tumor growth might be constrained by host tissue resistance if no space is released, as suggested by the suppression of tumorigenesis when tumor cells lack

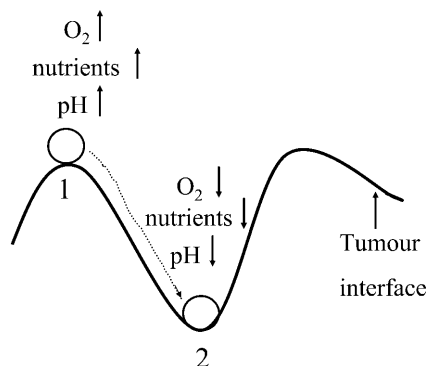


FIGURE 10 Cell surface diffusion. A schematic diagram of surface diffusion at the tumor border. A new cell born in 1 migrates until a neighboring position, 2, in which the local curvature of the interface is higher and the coordination number is greater than at its original position.

proper matrix metalloproteinases (Wilson et al., 1997) or when there is an increase in matrix proteins at the stroma-stroma border (Bleuel et al., 1999). In addition, a loss of tumorigenicity might occur if such a space is refilled with host cells more resistant to an acidic microenvironment. The fact that tumor cells transduced with certain cytokines lose their tumorigenicity by a mechanism involving a strong recruitment of neutrophils (Hirose et al., 1995; Musiani et al., 1996; Milella et al., 1999) supports this possibility. These cells are resistant to extracellular acidosis (Gukovskaya et al., 1992; Serrano et al., 1996) and may compete for space at the acidic host-tumor interface.

These pressure effects, as an inhibiting factor of tumor cell proliferation, are in good agreement with previous reports on solid state stress in tumor spheroids (Haji-Karim and Carlsson, 1978; Mueller-Klieser, 1997; Acker, 1998; Hamilton, 1998; Kunz-Schugart et al., 1998; Santini and Rainaldi, 1999). These spheroids are clusters of cancer cells that have been widely used in the laboratory to study the early stages of avascular tumor growth, the response to external factors such as supplied nutrients or growth inhibitory factors, cellular differentiation, and cell-cell interactions, and have even been used in therapeutically oriented studies. Helmlinger (1997) showed that solid stress inhibits their growth. The pressure exerted by the host over the tumor could explain the deviation of the tumor growth rate from a pure linear regime. This effect is not present in the two-dimensional in vitro cell colonies of our study, and this might be responsible for the pure linear regime of the growth rate even after very long periods (Fig. 10). Cell colonies in vitro should undergo a pure linear regime until they reach whole confluence.

In summary, this article shows that tumor cells of widely different genetic backgrounds share a common behavior. When tumors grow in vitro, this behavior is completely compatible with MBE universality dynamics. Further, there is sufficiently abundant and clear biological and clinical evidence to suggest that this is also the case in vivo, although further work is needed to confirm this. In any case, a universal tumor growth dynamics is observed for any type of tumor in vivo, independently of any other characteristic of tumoral cell lines. This dynamics is always governed by processes of cell surface diffusion. However, more work is needed to fully determine the whole dynamical behavior of tumor growth. The fractality of the contour of all the studied cell colonies and tumors has been demonstrated. Scaling techniques show that in vitro and in vivo cell proliferation would obey the same dynamics, independent of cell line or any other characteristic. These universal dynamics are compatible with a linear growth regime, a result in contrast with the currently accepted exponential or Gompertzian models of tumor growth. The main mechanism responsible for tumor progression, as for any cell proliferation process, is cell diffusion on the tumor border. These results incorporate the new concept that the major conditioner of tumor growth

is space competition between tumor and the host, which is more important than nutrient competition or angiogenesis, etc. The latter must be considered, in some cases, as necessary or as a coadjuvant condition of tumor growth, but their effects mainly consist of modifying the growth rate—perhaps simply allowing it or not. These results invalidate the current concept of cell proliferation and offer a unified view of tumor development. The dynamics involved provide coherent explanations where the traditional model cannot. Despite the importance of characteristics common to the dynamics of the in vivo growth of different tumors, more work is needed to completely characterize them. It should not be forgotten that, independent of interpretations, this article shows for the first time that different tumors have common characteristics such as the distribution of cell proliferation and their characteristic forms (that would imply common basic growth processes), determined via the critical exponents of local and global roughness.

As a result, some important features of cancer can be better explained. Moreover, some clinical strategies may need to be revised.

## APPENDIX A: SCALING ANALYSIS

In this procedure, the critical exponents are the so-called local roughness of the interface,  $\alpha_{loc}$ , the interface global roughness,  $\alpha_{glob}$ , the dynamic exponent,  $z$ , the growth exponent  $\beta$ , and the critical exponent  $\beta^*$ . These critical exponents originate as a result of the power law behavior of the geometry, and the development in time of the interface (tumor-host surface) (Brú et al., 1998). This power law behavior is associated with two quantities used in the description of tumor cell colonies. The first is the mean radius of the colony border:

$$\langle r \rangle = N^{-1} \sum_{i=1}^N r_i(t). \quad (3)$$

Its development over time gives the growth velocity of the tumor. The second is the rough aspect which can be quantified in terms of the standard deviation of the mean radius, denominated the width of the interface:

$$w(l, t) = \left\{ \frac{1}{N} \sum_{i=1}^N [r_i(t) - \langle r \rangle_1]^2 \right\}_L^{1/2}, \quad (4)$$

where  $\langle \cdot \rangle_1$  represents the local average of subsets of the arc of length  $l$  and  $\langle \cdot \rangle_L$  the average of the whole system. These fluctuations around the average position of the external cells of colonies grow in time in a power law fashion,  $w(l, t) \sim t^\beta$ , with a characteristic critical exponent  $\beta$ , the growth exponent. In the same manner, if we select small windows over the whole tumor, the larger the size of the window, the greater the width of the interface. These spatially growing fluctuations also follow a power law,  $w(l, t) \sim l \alpha_{loc}$ , with another characteristic exponent,  $\alpha_{loc}$ , the local roughness exponent, which can also be obtained from the scaling behavior of the correlation functions. The behavior described above cannot be used at all scales in a finite-size system such as a tumor because the fluctuations cannot grow indefinitely. Therefore, there must exist a point at which these temporal fluctuations saturate, a situation that is not common in systems with circular symmetry. This critical time is called the saturation time ( $t_s$ ) and its dependence with the

system size provides a new critical exponent: the dynamic exponent  $z$ . These results for the interface width can be summarized as follows (Barabási and Stanley, 1995):

$$w(l, t) = \begin{cases} t^\beta & \text{if } t \ll t_S \\ l^{\alpha_{loc}} & \text{if } t \gg t_S \end{cases} \quad (5)$$

The last magnitude used in this analysis was the spectrum of the tumor profiles. This quantity measures the characteristic length of interface structures formed by solid cell colonies in their growth process. Computing the power spectra as the Fourier transformation of the interface,  $h(x, t)$ , a power law behavior is established with an exponent referred to as global roughness,  $\alpha_{glob}$  (Barabási and Stanley, 1995; Brú et al., 1998; López et al., 1997):

$$S(k, t) = k^{-(2\alpha_{glob}+1)} s(kt^{1/z}), \quad (6)$$

where  $k$  is the momentum and  $s$  the structure factor.

None of these critical exponents are independent, but are related by the following:

$$z = \frac{\alpha_{glob}}{\beta} \quad (7)$$

and

$$\beta^* = \frac{\alpha_{glob} - \alpha_{loc}}{z}, \quad (8)$$

where  $\beta^*$  is another critical exponent. Therefore, the whole set of critical exponents that determine the dynamics of a growth process is  $\alpha_{loc}$ ,  $\alpha_{glob}$ ,  $\beta$ ,  $\beta^*$ , and  $z$ .

We thank Eliezer Shochat, José Antonio Cuesta, and Rodolfo Cuerno for fruitful discussions, Jesús Martín Tejedor for help, David Casero and Susana García for technical assistance, and Dirk Drasdo for reading the final manuscript. Our special thanks to Ysmael Alvarez and Granada Alvarez for time lapse video filming, and Luis Ortega for analyzing animal tissue sections.

## REFERENCES

- Abercrombie, M. 1979. Contact inhibition and malignancy. *Nature*. 281:259–262.
- Acker, H. 1998. The use of human tumour cells grown in multicellular spheroid culture for designing and improving therapeutic strategies. *J. Theor. Med.* 1:193–207.
- Barabási, A. L., and H. E. Stanley. 1995. *Fractal Concepts in Surface Growth*. Cambridge University Press, Cambridge.
- Bleuel, K., S. Popp, N. E. Fusenig, E. J. Stanbridge, and P. Boukamp. 1999. Tumor suppression in human skin carcinoma cells by chromosome 15 transfer or thrombospondin-1 overexpression through halted tumor vascularization. *Proc. Natl. Acad. Sci. USA*. 96:2065–2070.
- Brú, A., J. M. Pastor, I. Feraud, S. Melle, and I. Brú. 1998. Super-rough dynamics on tumour growth. *Phys. Rev. Lett.* 81:4008–4011.
- Byrne, H. M. 1997. The effect of time delays on the dynamics of avascular tumor growth. *Math. Biosci.* 144:83–117.
- Caratero, C., A. Hijazi, A. Caratero, C. Mazerolles, P. Rischmann, and J. P. Sarraon. 1990. Flow cytometry analysis of urothelial cell DNA content according to pathological and clinical data on 100 bladder tumors. *Eur. Urol.* 18:145–149.
- Claridge, E., P. Hall, and M. Keefe. 1992. Shape analysis for classification of malignant melanoma. *J. Biomed. Eng.* 14:229–234.
- Cross, S. S., A. J. C. McDonagh, T. J. Stephenson, D. W. Cotton, and J. C. Underwood. 1995. Fractal and integer-dimensional geometric analysis of pigmented skin lesions. *Am. J. Dermatopathol.* 17:374–378.
- Das Sarma, S., S. V. Ghaisas, and J. M. Kim. 1994. Kinetic super-roughening and anomalous dynamic scaling in nonequilibrium growth models. *Phys. Rev. E*. 49:122–125.
- Drasdo, D. 2000. Buckling instabilities in one-layered growing tissues. *Phys. Rev. Lett.* 84:4424–4427.
- Durand, R. E. 1990. Multicell spheroids as a model for cell kinetics studies. *Cell Tissue Kinet.* 23:141–159.
- Eden, M. 1961. Proceedings of the 4th Berkeley Symposium on Mathematics and Probability Vol. 4. J. Neyman, editor. University of California Press, Berkeley.
- Egeblad, M., and Z. Werb. 2002. New functions for the matrix metalloproteinases in cancer progression. *Nat. Rev. Cancer*. 2:163–176.
- Eskey, C. J., A. P. Koretsky, M. M. Domach, and R. K. Jain. 1993. Role of oxygen vs. glucose in energy metabolism in a mammary carcinoma perfused ex vivo: direct measurement by  $^{31}\text{P}$  NMR. *Proc. Natl. Acad. Sci. USA*. 90:2646–2650.
- Ferreira, S. C., Jr., M. L. Martins, and M. J. Vilela. 2002. Reaction-diffusion model for the growth of avascular tumor. *Phys. Rev. E*. 65:021907-1–021907-8.
- Fukakawa, N. 1997. Heterogeneity of DNA ploidy pattern in carcinoma of the gallbladder: primary and metastatic sites. *Jpn. J. Cancer Res.* 88: 886–894.
- Gatenby, R. A., and E. T. Gawlinsky. 1996. A reaction-diffusion model for cancer invasion. *Cancer Res.* 56:5745–5753.
- Gukovskaya, N. A., J. Tseng, and S. Grinstein. 1992. Activation of vacuolar-type proton pumps by protein kinase C. Role in neutrophil pH regulation. *J. Biol. Chem.* 267:22740–22746.
- Haji-Karim, M., and J. Carlsson. 1978. Proliferation and viability in cellular spheroids of human origin. *Cancer Res.* 38:1457–1464.
- Hamilton, G. 1998. Multicellular spheroids as an in vitro tumor model. *Cancer Lett.* 131:29–34.
- Harris, A. L. 2002. Hypoxia—a key regulatory factor in tumour growth. *Nat. Rev. Cancer*. 2:38–47.
- Hart, D., E. Shochat, and Z. Agur. 1998. The growth law of primary breast cancer as inferred from mammography screening trials data. *Br. J. Cancer*. 78:382–387.
- Helmlinger, G., P. A. Netti, H. C. Lichtenbeld, R. J. Melder, and R. K. Jain. 1997. Solid stress inhibits the growth of multicellular tumor spheroids. *Nat. Biotechnol.* 15:778–783.
- Hirose, K., M. Hakozi, Y. Nyunoya, Y. Kobayashi, K. Matsushita, T. Takenouchi, A. Mikata, N. Mukaida, and K. Matsushima. 1995. Chemokine gene transfection into tumour cells reduced tumorigenicity in nude mice in association with neutrophilic infiltration. *Br. J. Cancer*. 72:708–714.
- Kansal, A. R., S. Torquato, G. R. Harsh, E. A. Chiocca, and T. S. Deisboeck. 2000. Simulated brain tumor growth dynamics using a three-dimensional cellular automaton. *J. Theor. Biol.* 203:367–382.
- Kessler, D. A., H. Levine, and L. M. Sander. 1992. Molecular-beam epitaxial growth and surface diffusion. *Phys. Rev. Lett.* 69:100–103.
- Kunz-Schugart, L. A., M. Kreutz, and R. Knuechel. 1998. Multicellular spheroids: a three-dimensional in vitro culture system to study tumor biology. *Int. J. Exp. Pathol.* 79:1–23.
- Liberman, L., M. Drotman, E. A. Morris, L. R. La Trenta, A. F. Abramson, and M. F. Zakowski. 2000. Imaging-histologic discordance at percutaneous breast biopsy. *Cancer*. 89:2543–2546.
- López, J. M., M. A. Rodríguez, and R. Cuerno. 1997. Power spectrum scaling in anomalous kinetic roughening of surfaces. *Physica A*. 246:329–347.
- Losa, G. A. 1995. Fractals in pathology: are they really useful? *Pathologica*. 87:310–317.

- Losa, G. A., G. Baumann, and T. F. Nonnenmacher. 1992. Fractal dimension of pericellular membranes in human lymphocytes and lymphoblastic leukemia cells. *Pathol. Res. Pract.* 188:680–686.
- Mandelbrot, M. 1982. *Fractal Geometry of Nature*. Freeman, San Francisco.
- Milella, M., J. Jacobelli, F. Cavallo, A. Guarini, F. Velotti, L. Frati, R. Foa, G. Forni, and A. Santoni. 1999. Interleukin-2 gene transfer into human transitional cell carcinoma of the urinary bladder. *Br. J. Cancer.* 79: 770–779.
- Mueller-Klieser, W. 1997. Three-dimensional cell cultures: from molecular mechanisms to clinical applications. *Am. J. Physiol.* 273:C1109–C1123.
- Musiani, P., A. Allione, A. Modica, P. L. Lollini, M. Giovarelli, F. Cavallo, F. Belardelli, G. Forni, and A. Modesti. 1996. Role of neutrophils and lymphocytes in inhibition of a mouse mammary adenocarcinoma engineered to release IL-2, IL-4, IL-7, IL-10, IFN-alpha, IFN-gamma, and TNF-alpha. *Lab. Invest.* 74:146–157.
- Nicholson, G. L. 1987. Tumor instability, diversification and progression to the metastatic phenotype: from oncogene to oncofetal expression. *Cancer Res.* 47:1473–1487.
- Rasnack, D., and P. H. Duesberg. 1999. How aneuploidy affects metabolic control and causes cancer. *Biochem. J.* 340:621–630.
- Ried, T., K. Heselmeyer-Haddad, H. Blegen, E. Schrock, and G. Auer. 1999. Genomic changes defining the genesis, progression, and malignancy potential in solid human tumors: a phenotype/genotype correlation. *Gen. Chrom. Cancer.* 25:195–204.
- Santini, M. T., and G. Rainaldi. 1999. Three-dimensional spheroid model in tumor biology. *Pathobiology.* 67:148–157.
- Sato, H., T. Takino, Y. Okada, J. Cao, A. Shinagawa, E. Yamamoto, and M. Seiki. 1994. A matrix metalloproteinase expressed on the surface of invasive tumour cells. *Nature.* 370:61–65.
- Scalerandi, M., A. Romano, G. P. Pescarmona, P. P. Delsanto, and C. A. Condat. 1999. Nutrient competition as a determinant for cancer growth. *Phys. Rev. E.* 59:2206–2217.
- Serrano, C. V., Jr., A. Fraticelli, R. Panicia, A. Teti, B. Noble, S. Corda, T. Faraggiana, R. C. Ziegelstein, J. L. Zweier, and M. C. Capogrossi. 1996. pH dependence of neutrophil-endothelial cell adhesion and adhesion molecule expression. *Am. J. Physiol.* 271:962–970.
- Shackney, S. E. 1970. A computer model for tumor growth and chemotherapy and its application to L1210 leukemia treated with cytosine arabinoside (NSC-63878). *Cancer Chemother. Rep.* 54: 399–429.
- Shackney, S. E. 1993. *Tumor Growth, Cell Cycle Kinetics, and Cancer Treatment*. McGraw Hill, New York.
- Shackney, S. E., G. W. McCormack, and G. J. Cuchural. 1978. Growth rates of solid tumors and their relation to responsiveness to therapy. An analytical review. *Ann. Intern. Med.* 89:107–121.
- Sherrat, J. A., and M. A. J. Chaplain. 2001. A new mathematical model for avascular tumour growth. *J. Math. Biol.* 43:291–312.
- Skipper, H. E., F. M. Schabel, Jr., L. B. Mellet, J. A. Montgomery, L. J. Wilkoff, H. H. Lloyd, and R. W. Brockman. 1970. Implications of biochemical, cytogenetics, pharmacologic, and toxicologic relationships in the design of optimal therapeutic schedules. *Cancer Chemother. Rep.* 54:431–450.
- Sun, X. F., H. Ekberg, H. Zhang, J. M. Carstensen, and B. Nordenskjold. 1998. Overexpression of ras is an independent prognostic factor in colorectal adenocarcinoma. *APMIS.* 106:657–664.
- Tomita, T. 1995. DNA ploidy and proliferating cell nuclear antigen in colonic adenomas and adenocarcinomas. *Dig. Dis. Sci.* 40:996–1004.
- Wilson, C. L., K. J. Heppner, P. A. Labosky, B. L. Hogan, and L. M. Matrisian. 1997. Intestinal tumorigenesis is suppressed in mice lacking the metalloproteinase matrilysin. *Proc. Natl. Acad. Sci. USA.* 94: 1402–1407.